Article

Electrostatic Control of Thickness and Stiffness in a Designed Protein Fiber

David Papapostolou, Elizabeth H. C. Bromley, Christopher Bano, and Derek N. Woolfson

J. Am. Chem. Soc., **2008**, 130 (15), 5124-5130 • DOI: 10.1021/ja0778444 • Publication Date (Web): 25 March 2008

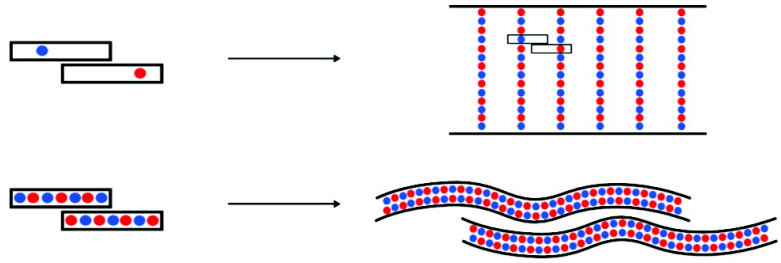

J|A|C|S
ARTICLES

Published on Web 03/25/2008

Electrostatic Control of Thickness and Stiffness in a Designed Protein Fiber

David Papapostolou,[†] Elizabeth H. C. Bromley,[†] Christopher Bano,[†] and Derek N. Woolfson*[,†,‡]

School of Chemistry, University of Bristol, Cantock's Close, Bristol BS8 1TS, U.K., and Department of Biochemistry, University of Bristol, University Walk, Bristol BS8 1TD, U.K.

Received October 12, 2007; E-mail: D.N.Woolfson@bristol.ac.uk

Abstract: Attempts to design peptide-based fibers from first principles test our understanding of protein folding and assembly, and potentially provide routes to new biomaterials. Several groups have presented such designs based on α-helical and β-strand building blocks. A key issue is this area now is engineering and controlling fiber morphology and related properties. Previously, we have reported the design and characterization of a self-assembling peptide fiber (SAF) system based on α-helical coiled-coil building blocks. With preceding designs, the SAFs are thickened, highly ordered structures in which many coiled coils are tightly bundled. As a result, the fibers behave as rigid rods. Here we report successful attempts to design new fibers that are thinner and more flexible by further programming at the amino-acid sequence level. This was done by introducing extended, or "smeared", electrostatic networks of arginine and glutamate residues to the surfaces of the coiled-coil building blocks. Furthermore, using arginine—rather than lysine—in these networks plays a major role in the fiber assembly, presumably by facilitating multidentate intra and intercoiled-coil salt bridges.

Introduction

The de novo design of bioinspired fibrous materials is challenging, but has potential applications in nanobiotechnology, which range from ordered arrays for nanoelectronics to three-dimensional (3D) scaffolds for tissue engineering.[1–3] Indeed, considerable effort has been made to develop new self-assembling systems based on nucleic acids, peptides, and proteins.[1–4] Through this work, impressive arrays of discrete nanoscale objects and nano-to-mesoscale biomaterials have been constructed. However, and particularly for peptide- and protein-based materials, programming and controlling the morphology (shape, size, and related physical properties) of such materials has proven difficult.

Regarding peptide-based fibrous assemblies,[1–3] many of these are based on β-structured peptide assemblies, or amyloid-like structures,[1,5,6] and will not be discussed in detail in this paper. The α-helix has also proven to be a valuable building block, or *tecton,*[7] for constructing fibrous biomaterials de novo, and this has spawned a rapidly growing subfield;[8–14] this area has been reviewed recently.[3] The leucine-zipper motif, which is a specific type of dimeric α-helical coiled coil, has been particularly exploited in this area. Leucine zippers (LZs) make ideal tectons for nanoscale assemblies and nanostructured biomaterials for several reasons: LZs are among the most straightforward and best-understood peptide–peptide interaction motifs;[15] as a result, reliable rules for LZ design and assembly are available;[16] LZs are small motifs (∼30 amino acids long) that are synthetically accessible; when folded, LZs have the approximate dimensions of 4 nm × 2 nm cylinders; and finally, building with LZs is scalable, that is, tandem LZ repeats (which can be noncovalently assembled or covalently linked) can be used to generate structures that span the nanometer or micrometer regimes, but still reflect the underlying nanoscale tectons.[7,16,17]

[†] School of Chemistry.
[‡] Department of Biochemistry.

(1) MacPhee, C. E.; Woolfson, D. N. *Curr. Opin. Solid State Mater. Sci.* **2004**, *8*, 141–149.
(2) Fairman, R.; Akerfeldt, K. S. *Curr. Opin. Struct. Biol.* **2005**, *15*, 453–463.
(3) Woolfson, D. N.; Ryadnov, M. G. *Curr. Opin. Chem. Biol.* **2006**, *10*, 559–567.
(4) Jaeger, L.; Chworos, A. *Curr. Opin. Struct. Biol.* **2006**, *16*, 531–543.
(5) Zhang, S. G.; Marini, D. M.; Hwang, W.; Santoso, S. *Curr. Opin. Chem. Biol.* **2002**, *6*, 865–871.
(6) Rajagopal, K.; Schneider, J. P. *Curr. Opin. Struct. Biol.* **2004**, *14*, 480–486.
(7) Bromley, E. H. C.; Channon, K.; Moutevelis, E.; Woolfson, D. N. *ACS Chem. Biol.* **2008**, *3*, 38–50.
(8) Kojima, S.; Kuriki, Y.; Yoshida, T.; Yazaki, K.; Miura, K. *Proc. Jpn. Acad., Ser. B* **1997**, *73*, 7–11.
(9) Pandya, M. J.; Spooner, G. M.; Sunde, M.; Thorpe, J. R.; Rodger, A.; Woolfson, D. N. *Biochemistry* **2000**, *39*, 8728–8734.
(10) Potekhin, S. A.; Melnik, T. N.; Popov, V.; Lanina, N. F.; Vazina, A. A.; Rigler, P.; Verdini, A. S.; Corradin, G.; Kajava, A. V. *Chem. Biol.* **2001**, *8*, 1025–1032.
(11) Zimenkov, Y.; Conticello, V. P.; Guo, L.; Thiyagarajan, P. *Tetrahedron* **2004**, *60*, 7237–7246.
(12) Frost, D. W. H.; Yip, C. M.; Chakrabartty, A. *Biopolymers* **2005**, *80*, 26–33.
(13) Lazar, K. L.; Miller-Auer, H.; Getz, G. S.; Orgel, J.; Meredith, S. C. *Biochemistry* **2005**, *44*, 12681–12689.
(14) Wagner, D. E.; Phillips, C. L.; Ali, W. M.; Nybakken, G. E.; Crawford, E. D.; Schwab, A. D.; Smith, W. F.; Fairman, R. *Proc. Natl. Acad. Sci. U.S.A.* **2005**, *102*, 12656–12661.
(15) Mason, J. M.; Arndt, K. M. *ChemBioChem* **2004**, *5*, 170–176.
(16) Woolfson, D. N. *Adv. Protein Chem.* **2005**, *70*, 79–112.
(17) Ryadnov, M. G.; Woolfson, D. N. *J. Am. Chem. Soc.* **2007**, *129*, 14074–14081.

 10.1021/ja0778444 CCC: $40.75

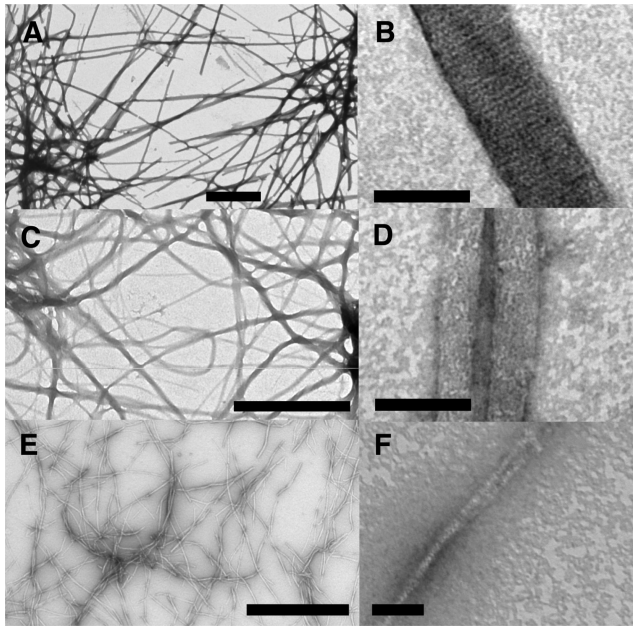

Figure 1. Transmission electron micrographs of standard SAFs (A and B), the SAF-SC-4 (C and D) and SAF-SC-3 (E and F) fibers, stained with 1% uranyl acetate. (A, C, and E): low-magnification images (scale bars: 1 μm); (B, D, and F): high-magnification images (scale bar: 50 nm).

Previously, we have reported the design, assembly, and experimental characterization of a new class of fibrous biomaterials based on LZ peptides 28-residues long.[9] In this so-called self-assembling fiber (SAF) system, two complementary LZ peptides are designed to coassemble to form sticky-ended dimers which, in turn, are engineered to foster end-to-end assembly into long, noncovalently linked α-helical coiled-coil fibrils. In practice, and through some as yet undetermined mechanism, these fibrils bundle to form stiff, thickened fibers (Figure 1A and B). The final dimensions of these matured fibers are ~40 nm thick and 1–15 μm long. The fibers behave as stiff rods that do not bend over their entire lengths; therefore, their persistence lengths must be greater than the experimentally observed lengths, that is, >15 μm.[18]

Over the past five years, we have reported redesigned and engineered SAF systems with improved stability,[19,20] of altered fiber morphology and general properties,[19,21,22] and with appended functions.[18,23] Most significantly for the work presented here, however, we have described the subtle redesign of the first-generation SAFs,[9] to give more stable and better ordered second-generation SAFs. The redesign process rests on the simple assumption that the outer surfaces of the coiled-coil fibrils interact somehow to give thickening, with the focus on potential charge–charge interactions. Specifically, discrete, complementary charge clusters are introduced to the surfaces of the interacting coiled coils—namely, a pair of negatively charged aspartates on one peptide, to complement an identically spaced pair of positively charged arginine side chains on the other.[20] This promotes further thickening (to give ~70 nm fibers), and improves assembly and thermal stability. Interestingly, matured second-generation fibers also display considerable internal order, observed as sharp patterns by X-ray fiber diffraction, and regular striations on the outer surfaces in TEM (Figure 1B).[24] Moreover, the striation pattern precisely matches the ~4.2 nm length expected for the folded LZ tectons. These recent data indicate that the introduced interfibril charge–charge interactions are acting as designed to specify fibril−fibril interactions.[24]

These particular properties distinguish the SAFs from some of the other coiled-coil-based peptide−fiber systems, which show thickening, but with little or no apparent internal organization and ultrastructure;[3,11,14,25,26] similar ripening behavior has also been observed for recently engineered self-assembled collagens.[27–29]

Our successes in the design and redesign of the SAF system and the useful, albeit serendipitous, discovery of fiber thickening encouraged us to probe thickening further. As described herein, we have attempted to create thinner and more flexible peptide fibers. We show that this can be done by further programming charge–charge interactions on the surfaces of the underlying coiled-coil units. Specifically, the surfaces were supercharged to make them highly hydrophilic with smeared, rather than discrete, charged patches. As a result fibers can be thinned down to ~10 nm and made much more flexible such that they wrap around one another to form loose, but nongelling, networks. The redesigns come at a price, however, as some fiber stability and the internal order appear to have been lost.

Ionic- and polyelectrolyte-based self-assemblies are well established in the preparation of both hard and soft multicomponent, nanostructured materials. Indeed, the depth and breadth of these fields preclude a detailed survey here. Instead, we refer the reader to excellent reviews by others.[30–34] In short, the approaches taken employ simplexes, layer-by-layer deposition, the self- and coassembly of block copolymers, and polyelectrolyte−amphiphile interactions. By and large, these center on combining molecules of opposite charge, i.e., either all anionic or all cationic. The approach outlined herein, although it adds to this effort in some respects, is distinct in that we have rationally designed folded peptide structures that present faces

(18) Smith, A. M.; Acquah, S. F. A.; Bone, N.; Kroto, H. W.; Ryadnov, M. G.; Stevens, M. S. P.; Walton, D. R. M.; Woolfson, D. N. *Angew. Chem., Int. Ed.* **2004**, *44*, 325–328.
(19) Ryadnov, M. G.; Woolfson, D. N. *Nat. Mater.* **2003**, *2*, 329–332.
(20) Smith, A. M.; Banwell, E. F.; Edwards, W. R.; Pandya, M. J.; Woolfson, D. N. *Adv. Funct. Mater.* **2006**, *16*, 1022–1030.
(21) Ryadnov, M. G.; Woolfson, D. N. *Angew. Chem., Int. Ed.* **2003**, *42*, 3021–3023.
(22) Ryadnov, M. G.; Woolfson, D. N. *J. Am. Chem. Soc.* **2005**, *127*, 12407–12415.
(23) Ryadnov, M. G.; Woolfson, D. N. *J. Am. Chem. Soc.* **2004**, *126*, 7454–7455.
(24) Papapostolou, D.; Smith, A. M.; Atkins, E. D. T.; Oliver, S. J.; Ryadnov, M. G.; Serpell, L. C.; Woolfson, D. N. *Proc. Natl. Acad. Sci. U.S.A.* **2007**, *104*, 10853–10858.
(25) Kajava, A. V.; Potekhin, S. A.; Corradin, G.; Leapman, R. D. *J. Pept. Sci.* **2004**, *10*, 291–297.
(26) Zimenkov, Y.; Dublin, S. N.; Ni, R.; Tu, R. S.; Breedveld, V.; Apkarian, R. P.; Conticello, V. P. *J. Am. Chem. Soc.* **2006**, *128*, 6770–6771.
(27) (a) Paramonov, S. E.; Gauba, V.; Hartgerink, J. D. *Macromolecules* **2005**, *38*, 7555–7561. (b) Rele, S.; Song, Y.; Apkarian, R. P.; Qu, Z.; Conticello, V. P.; Chaikof, E. L. *J. Am. Chem. Soc.* **2007**, *129*, 14780–14787.
(28) Koide, T.; Homma, D. L.; Asada, S.; Kitagawa, K. *Bioorg. Med. Chem. Lett.* **2005**, *15*, 5230–5233.
(29) Kotch, F. W.; Raines, R. T. *Proc. Natl. Acad. Sci. U.S.A.* **2006**, *103*, 3028–3033.
(30) Faul, C. F. J.; Antonietti, M. *Adv. Mater.* **2003**, *15*, 673–683.
(31) Stuart, M. A. C.; Hofs, B.; Voets, I. K.; de Keizer, A. *Curr. Opin. Colloid Interface Sci.* **2005**, *10*, 30–36.
(32) Johnston, A. P. R.; Cortez, C.; Angelatos, A. S.; Caruso, F. *Curr. Opin. Colloid Interface Sci.* **2006**, *11*, 203–209.
(33) Harada, A.; Kataoka, K. *Prog. Polym. Sci.* **2006**, *31*, 949–982.
(34) Hales, K.; Pochan, D. J. *Curr. Opin. Colloid Interface Sci.* **2006**, *11*, 330–336.

Table 1. SAF-SuperCharged Peptide Sequences

Peptide	Sequence and coiled-coil register
	gabcdef gabcdef gabcdef gabcdef
C3A	EIRRLEE EIRRLEE ENRRLEY
C3B	RNEELRY RIEELRR RIEELRR
C4A	EIRRLEE EIRRLEE EIRRLEE ENRRLEY
C4B	RIEELRR RNEELRY RIEELRR RIEELRR
C3AK	EIKKLEE EIKKLEE ENKKLEY
C3BK	KNEELKY KIEELKK KIEELKK
C4AK	EIKKLEE EIKKLEE EIKKLEE ENKKLEY
C4BK	KIEELKK KNEELKY KIEELKK KIEELKK

that incorporate both anionic and cationic charges to alter the higher-order assembly of the peptide blocks.

Results and Discussion

Peptide Design. The SAF-SuperCharged (SAF-pSC) peptides described herein (see Table 1 for peptide sequences) follow sticky-end design principles similar to those reported elsewhere (Figure 2).[9] Briefly, the self-assembly fiber (SAF) peptides are based on the heptad repeat associated with coiled-coil protein sequences. This is often denoted ***abcdefg*** with hydrophobic residues at the ***a*** and ***d*** sites, which form the hydrophobic core of the coiled-coil helical bundle. Good design rules are now available for coiled-coil structures.[16] For example, the combination of isoleucine at ***a*** and leucine at ***d*** best specifies dimeric leucine zippers (LZs). The helical interface can be cemented further with interhelical (intracoiled coil) charge–charge interactions between successive ***g*** and ***e*** sites. Together these rules give the general framework of +IxxL-x (in a ***gabcdef*** register) for a LZ sequence; where x is usually made a polar residue or alanine. Tandem repeats of 3–5 such heptads tend to associate to give stably folded structures. Further specificity can be achieved, although at the expense of some stability, by incorporating hydrogen-bond-forming pairs of asparagine sides at ***a*** sites in the hydrophobic core. A combination of such asparagine residues at offset ***a*** sites, and complementary interhelical charges was used to achieve the sticky-ended heterodimer designed to propagate the SAFS.

In addition to the above considerations, two other design principles were incorporated into the new SAF-pSC peptides: first, after the heterodimeric Velcro system reported by O'Shea and Kim,[35] complementary, interhelical (intracoiled coil) charge–charge interactions were introduced by making all of the ***e*** and ***g*** positions of one peptide basic, and those of the other, acidic (Figure 2). Thus, for the basic SAF-pSC peptides, C3B and C4B, arginine was placed at every ***e*** and ***g*** position; while their acidic partners, C3A and C4A, had glutamate at all these sites. Second, to make the resulting coiled coils as soluble as possible, and introduce controllable aggregation, charged residues were placed at the ***b***, ***c*** and ***f*** positions of the coiled-coil repeat, i.e., on the outmost surfaces of the coiled coils. To avoid intrahelical repulsions, we introduced these to allow interconnected networks of intrahelical salt bridges by maximizing the i to i+3 and i to i+4 juxtapositions of oppositely charged side chains (Figure 2). This follows the work of Burkhard and colleagues who present a 2-heptad-long oligomerizing coiled-coil-like peptide bearing similar networks of intra- and intermolecular salt bridges.[36–38] Finally, two parent, two-peptide systems were designed, SAF-SuperCharged3 (C3) and SAF-SuperCharged4 (C4), differing by the length of the peptides: the C4 peptides were four-heptads, or 28-residues long, while the C3 peptides were shorter by one heptad. Using these design principles, we aimed to follow on from our work on the SAF system,[20,24] to further understand the phenomena of fiber thickening and order, and to attempt to design thinner, more-flexible fibers.

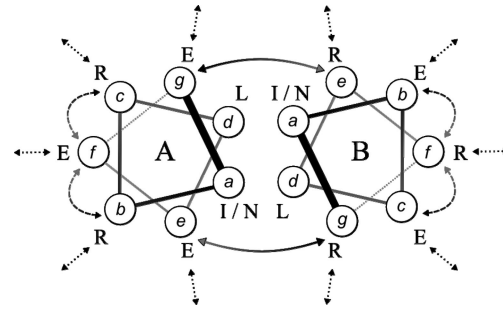

Figure 2. Design principles for the SAF-pSC peptides. Helical-wheel representation of the heptad repeats for the A- and B-series peptides. Potential salt bridges are shown: interhelical (solid arrows); intrahelical (dashed arrows); intercoiled coil (dotted arrows).

Visualizing SAF-SuperCharged Fibers by Electron Microscopy. Consistent with the design principles, when peptides C4A and C4B were mixed and incubated at 20 °C overnight (in 10 mM MOPS, pH 7.5), fibers were observed using negative-stain Transmission Electron Microscopy (TEM), Figures 1 C and D. In contrast, the individual peptides gave only amorphous aggregates (data not shown). The resulting C4A + C4B fibers were 2 to 3 times thinner than the standard SAFs, Figures 1 A and B, with average widths $\sim$ 25 nm (24.7 $\pm$ 4.9 nm; n = 113 measurements) compared with 43 $\pm$ 9.3 nm for the first-generation SAFs, and 69 $\pm$ 18.5 nm for second-generation SAFs.[20] Assuming that the influence of the core coiled-coil residues—i.e., those at ***a, d, e*** and ***g***—is minimal, this suggests that the charge distribution on the outer surface of component coiled-coil fibrils is indeed a key feature in fiber thickening,[20,24] and that fiber width can be programmed either way (thicker or thinner) within the peptide sequence.

Interestingly and in contrast to the standard SAFs, the C4A + C4B fibers were flexible, and appeared to lack internal order as judged by the absence of the aforementioned striation patterns in the stained TEM images (Figures 1B and D). Nonetheless, individual fibers did interact with each other to form loose bundles of two or three fibers (Figure 2C and D), and interconnected into networks. As a result, though individual fibers did not exceed 5 μm, these intertwined structures were 10 – 15 μm in length. This behavior is more reminiscent of the entangled polymers,[39] rather than the discrete rod-behavior typically observed for the standard SAFs.

Fibers were also observed for the mixture of the shorter, C3A and C3B, peptides (Figures 1E and F). These were shorter and

(35) O'Shea, E. K.; Lumb, K. J.; Kim, P. S. *Curr. Biol.* **1993**, *3*, 658–667.
(36) Burkhard, P.; Meier, M.; Lustig, A. *Protein Sci.* **2000**, *9*, 2294–2301.
(37) Burkhard, P.; Ivaninskii, S.; Lustig, A. *J. Mol. Biol.* **2002**, *318*, 901–910.
(38) Meier, M.; Lustig, A.; Aebi, U.; Burkhard, P. *J.Struct. Biol.* **2002**, *137*, 65–72.
(39) Jones, R. A. *Soft Condensed Matter*; Oxford University Press:New York, 2002; pp 90–91.

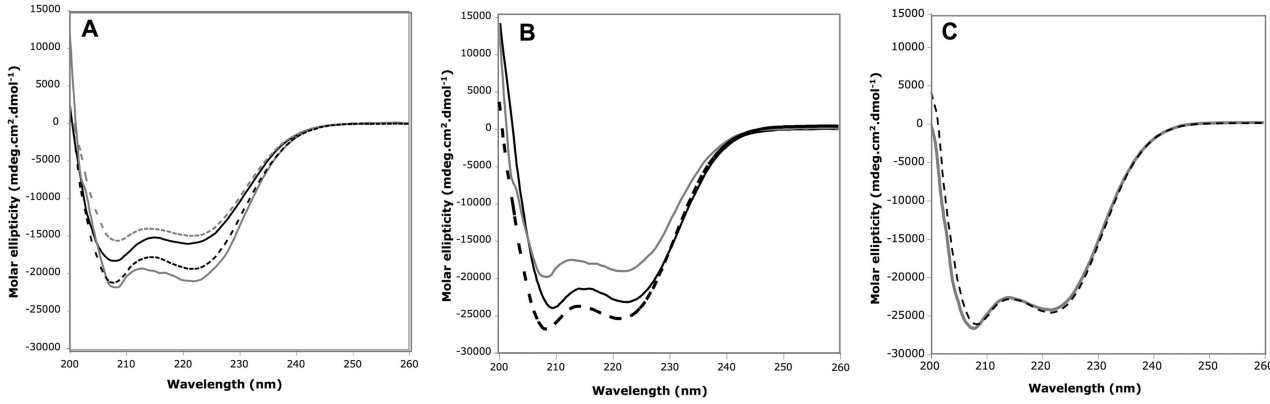

Figure 3. Circular dichroism spectra of the SAF-pSC4 peptides. (A) Individual peptides and mixtures: 100 μM C4A (black broken line); 100 μM C4B (gray broken line); C4A + C4B mixtures at 10 μM (gray solid line) and 100 μM in each peptide (black solid line). (B) C4A + C4B mixtures: 10 μM in each peptide and unperturbed (gray solid line); supernatant spun-down from a sample 100 μM in each peptide (black solid line); and 100 μM in each peptide and incubated with 300 mM KCl (black broken line). (C) C4A + C4B mixture incubated with 300 mM KCl (broken line), and an untreated C4AK + C4BK mixture (solid line); for these experiments all peptides were at 100 μM.

thinner than the C4A + C4B fibers (average length, 989 nm ± 318 nm; width, 10.7 nm ± 1.3 nm; $n = 54$). The tendency of C3A+C3B fibers to interact and to form networks was also increased (Figure 1E). Indeed, the shorter system in particular is reminiscent of entangled fibrous networks formed by amyloidogenic peptides,[40–42] which are based on β-sheet structures. The fibers made from the shorter peptides showed an increased tendency to be damaged by the electron beam, which made it difficult to collect very high-magnification images. We propose that this, together with the thinner fibers that the C3 peptides form, is related to the less-extensive—and, therefore less stabilizing—overhang in the designed sticky-ended dimers compared with those for the longer C4 system.

Despite the apparent wrapping and entanglement of fibers, neither SAF-pSC mixture formed gels at any concentration tested. This suggests that the fibers do not branch, or otherwise form noncovalently cross-linked networks.

The absence of striations, and therefore the apparent lack of internal order in the supercharged SAFs compared with our recently described second-generation fibers,[24] is interesting and noteworthy. Our contention is that this is consistent with our design principles as follows. The second-generation fibers have a relatively small number of charged residues on their outer surfaces, which are otherwise alanine and glutamine rich. Moreover, and compared with the first-generation SAFs, the charged residues are paired and placed such that they can potentially form a complementary, self-solvating, local, elelctrostatic networks within the matured fibers. By contrast the entire surfaces of the SAF-pSC coiled coils have charged side chains. We posit that: (1) this makes them difficult to completely desolvate; therefore, we anticipate that the fibers formed are internally wet and (2) that multiple, isoenergetic intercoiled-coil interactions can be made within these fibers, compared with the second-generations SAFs where more specific intercoiled-coil interactions should be made. These increased possibilities in the SAF-pSC system should not lead to thicker fibers, however, as thickening would increasingly incur the desolvation penalty, and/or other penalties associated with removing water from bulk.

Solution-Phase Characterization of SAF-pSC Mixtures. Circular dichroism (CD) spectroscopy is usually the technique of choice to study the folding of peptides into α-helical structures. Indeed, the CD spectra of SAF-pSC3 and SAF-pSC4 mixtures were typical of α-helices, as characterized by double minima at 208 and 222 nm (Figure 3). Nonetheless, this was curious as all other SAFs—as well helical fibers presented by others—show distorted α-helical spectra in which signals are attenuated, particularly the 208 nm signal, and red-shifted.[9] These are the hallmarks of light scattering associated with large and sometimes chiral assemblies in solution. This suggested subtly different assemblies in the SAF-pSC systems compared with the previous generations. Possibilities are that the thinner fibers simply do not scatter as much light, or that both the individual peptides and the mixtures fold to α-helical structures of some type. To test these two possibilities, the CD spectra of the individual peptides and mixtures were recorded under different conditions as follows.

First, under similar conditions used to study the C4A + C4B mixture, the individual SAF-pSC4 peptides, C4A and C4B, were also folded as α-helices with percentage α-helix calculated from the molar ellipticity values at 222 nm of ~60% and ~50%, respectively (Figure 3A). This autonomous folding probably reflects the high helix propensities of the peptides; their potential to form coiled-coil oligomers, despite these being noncognate (not designed) homo-oligomers; and the large number of potential $i, i + 3$ and $i, i + 4$ intrahelical salt bridges within the sequences. Again, both spectra were typical of α-helices (albeit partially folded), with no indication of β-sheet. Furthermore, C4A alone was found to be more helical than the SAF-pSC4 mixture (Figure 3A), suggesting that peptide assembly and/or the subsequent fiber growth resulted in a loss of CD signal. This led us to study the CD signal of peptide mixtures under (nonpermissive) conditions that did not lead to fiber growth as judged by TEM: namely, concentrations below 50 μM in each peptide, or salt concentrations above 50 mM KCl.

[*n.b.* A range of salt concentrations was explored from 0.5 to 500 mM KCl. Fibers were only observed by negative-stain TEM at 50 mM KCl or below. Under these permissive

(40) Lamm, M. S.; Rajagopal, K.; Schneider, J. P.; Pochan, D. J. *J. Am. Chem. Soc.* **2005**, *127*, 16692–16700.
(41) Papanikolopoulou, K.; Schoehn, G.; Forge, V.; Forsyth, V. T.; Riekel, C.; Hernandez, J. F.; Ruigrok, R. W. H.; Mitraki, A. *J. Biol. Chem.* **2005**, *280*, 2481–2490.
(42) Baldwin, A. J.; Bader, R.; Christodoulou, J.; MacPhee, C. E.; Dobson, C. M.; Barker, P. D. *J. Am. Chem. Soc.* **2006**, *128*, 2162–2163.

conditions fiber morphology (thickness and length) did not change appreciably within the experimental ranges given above. Though high, 300 mM KCl was used in the experiments described below because (1) fibers did not form, and (2) the CD signals for the individual and mixed peptides showed plateaus at this concentration.]

First of all, a nonpermissive, 10 μM mixture of SAF-pSC4 peptides showed a larger α-helical content than the more-concentrated, fiber-producing mixtures (Figure 3B). This indicated that fiber growth, but not the coiled-coil assembly, was responsible for the loss of signal described above and is consistent with previous CD data on the SAF systems. To investigate this further, a C4A + C4B fiber-containing mixture (at 100 μM in each peptide) was spun down by centrifugation, and a CD spectrum of the supernatant measured and normalized against the measured peptide concentration, which was found to be close to a third of the initial peptide concentration (~60 μM total peptide). The molar ellipticity of this supernatant was similar to that for an unperturbed, nonpermissive mixture of C4A + C4B (10 μM in each peptide) (Figure 3B).

These experiments demonstrate that peptides incorporated into grown fibers are not soluble and do not contribute fully to the CD signal, hence, the apparent drop in signal upon fiber formation. As a result, we conclude that, in the case of the SAF-pSC system at least, the CD signal does not report on the peptides incorporated in the fibers, but on smaller assemblies that are found in the supernatant of the spun-down fiber preparations. This latter point and the secondary structure of the peptides incorporated into fibers are addressed in the next two sections.

Before leaving this section, we are aware that the CD data for the SAF-pSC and standard SAF systems are possibly in conflict. Though, we note that the loss of signal observed for the SAF-pSC mixtures could be attributed to partial attenuation of the CD signal akin to that observed for the standard SAFs. More likely, however, the behavior is related to the ability shown by the SAF-pSC fibers to bundle into large networks that are more particulate than soluble proteins. In such heterogeneous systems artifacts can arise in CD spectra from the effects of differential light scattering and absorption flattening. By contrast, the standard SAFs form discrete rigid rods that do not appear to interact in solution or to form networks. In addition, the individual standard SAF peptides are much less folded than the individual SAF-pSC peptides and contribute much less to the solution-phase CD signal.[9]

Oligomerization of the SAF-pSC Peptides by Analytical Ultracentrifugation. To investigate the solution-phase assembly of the SAF-pSC peptides further, we turned to analytical ultracentrifugation (AUC).

First, as shown in Figure 4, data were recorded at a rotor speed of 3000 rpm. At this speed only very large assemblies sediment, and small oligomers of peptides of the mass of the SAF peptides do not. The sums of the traces for the individual peptides, which serve as controls, are superimposed on those for the experimental mixtures. Comparison of the traces for the individual peptides and fiber-forming mixtures of C4A and C4B (100 μM in each peptide and without salt) indicated a loss of approximately two-thirds of the peptide from solution, and a build up of aggregated material at large radii, Figure 4A. These data are fully consistent with the aforementioned CD analysis of the permissive C4 mixtures. In comparison, the data for C4A + C4B with 300 mM KCl—which is nonpermissive for fibers as judged by TEM—showed only a third of the signal is lost,

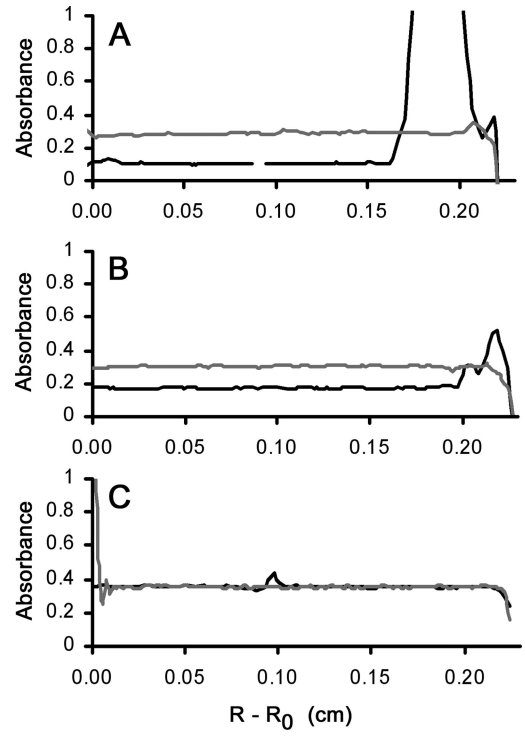

Figure 4. Low speed Analytical Ultracentrifugation of the SAF-pSC-4 and SAF-pSC-4K peptides (3000 rpm). (A) Average of 100 μM C4A and 100 μM C4B (gray line), 100 μM C4A + 100 μM C4B mixture (black line). (B) Average of 100 μM C4A and 100 μM C4B with 300 mM KCl (gray line), 100 μM C4A + 100 μM C4B mixture with 300 mM KCl (black line). (C) Average of 100 μM C4AK and 100 μM C4BK (gray line), 100 μM C4AK + 100 μM C4BK mixture (black line). Traces were aligned using the outer meniscus's.

and less signal from aggregated material at the bottom of the cell, Figure 4B.

To probe the oligomer states of the α-helical species that remained in solution further, we ran a series of conventional equilibrium AUC experiments at high rotor speeds, at which small LZ oligomers are known to sediment. For example, Figure 5 shows traces for the individual peptides and mixtures at a speed of 53000 rpm. These data indicate that for all samples the soluble peptides formed mixtures of small oligomers. The masses of C4A, C4B, the theoretical heterodimer and an averaged trimer are 3757, 3838, 7595 and 11392 Da, respectively. Without salt the global single ideal species fits to the data for C4A, C4B and the mixture were found to be 4458, 6391 and 8256 Da, respectively, Figure 5A. With 300 mM salt these increased to 6768, 8075 and 8510 Da, respectively, Figure 5B. This analysis indicates that the individual C4A and C4B peptides show varying propensities to self-associate into small oligomers, but not larger structures; and, for the mixtures, the peptides remaining in solution after fiber formation also form small oligomers. The apparent increase in solution-phase molecular weight with salt presumably reflects (1) a reduction in the electrostatic repulsion between peptides through additional screening of charge, and/or (2) an increase in the hydrophobic effect. Given the likely heterogeneity in these samples from the various associated states possible, we chose not to fit the AUC data to more-elaborate models for self-associating systems; besides, judging by the residuals, Figure 5, the fits to single ideal species were good, albeit for nonstoichiometric oligomers.

Structure in the Sedimented Fibers by ATR-FTIR. Taken together, the TEM, CD and AUC data show that while the SAF-

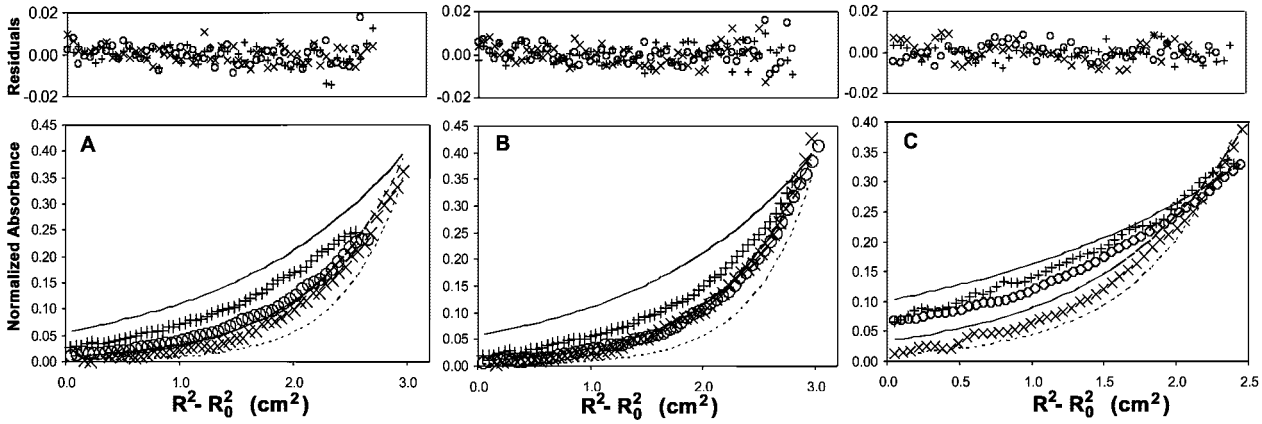

Figure 5. High-speed analytical ultracentrifugation of the SAF-pSC-4 and SAF-pSC-4K peptides (53000 rpm) with residuals from the single ideal species fit. (A) SAF-pSC-4 samples without KCl: 100 μM C4A (+), 100 μM C4B (○), 100 μM C4A + 100 μM C4B mixture (×), theoretical average monomer (solid line), theoretical average dimer (dashed line), theoretical average trimer (dotted line). (B) SAF-pSC-4 samples with 300 mM KCl. 100 μM C4A (+), 100 μM C4B (○), 100 μM C4A + 100 μM C4B mixture (×), theoretical average monomer (solid line), theoretical average dimer (dashed line), theoretical average trimer (dotted line). (C) SAF-pSC-4K samples with no salt. 100 μM C4AK (+), 100 μM C4BK (○), 100 μM C4AK + 100 μM C4BK mixture (×), theoretical average monomer (solid line), theoretical average dimer (dashed line), theoretical average trimer (dotted line).

pSC4 peptides have a strong tendency to combine to form helical oligomers in solution, these only propagate fibers in low salt and above a critical concentration in the 50 – 80 μM range, as judged by the observation of fibers by TEM over a range of peptide concentrations. A remaining question is, what is the dominant secondary structure in the sedimented fibrous form of the SAF-pSC mixtures? To be sure that the SAF-pSC systems were α-helical as designed, we used ATR-FTIR to probe the secondary structure of the SAF-pSC3 and SAF-pSC4 mixtures. Fiber preparations were spun-down and the fiber-containing pellets analyzed. ATR-FTIR spectra for fibers from both mixtures showed bands in the amide I and amide II regions typical of α-helices (Figure 6A);[43,44] specifically, the main component was close to 1650 cm^{-1}. Furthermore, the signal in the amide I region—a broad peak with 3–5 components—indicated coiled-coil assemblies (Figure 6B).[45] Moreover, the component at 1630 cm^{-1}, which can be confused with a strong peak centered at 1620 cm^{-1} typical of β-strands, was not a significant component in the SAF-pSC data. These data strongly support α-helical coiled-coil formation by the SAF-pSC systems, consistent with foregoing SAF designs and characterization using multiple techniques.[9,24]

Probing the Electrostatic Interaction Network. The TEM, CD, and AUC experiments of the SAF-pSC systems in salt—which show that salt disrupts fiber assembly—lends strong support to the hypothesis that intercoiled-coil salt bridges do contribute to fiber formation. However, the resulting fibers are thinner and more flexible than the foregoing SAF designs, indicating the competing effect of surface solubility. These observations are all consistent with the design hypothesis, though the SAF-pSC designs have not achieved the potential limit of single coiled-coil fibrils, which would have diameters of ∼2 nm. To probe the nature of the electrostatic interactions in both the soluble helical assemblies and the fibers further, we replaced all of the arginine residues in the C3 and C4 peptides with lysine. Here the aim was to test whether arginine exclusively promoted multiple electrostatic interactions and intercoiled-coil interactions better than lysine: in principle, the arginine-to-lysine mutations should reduce the salt-bridge and hydrogen-bonding potential of the basic side chains of the peptides, as lysine has only a primary amine moiety, whereas arginine has a guanidino group that can potentially form multiple interactions.[46–50]

The resulting pairs of peptides were named C3AK and C3BK and C4AK and C4BK, Table 1. Interestingly, neither of the arginine-to-lysine mutant systems formed fibers at 5 or 20 °C under our standard conditions as judged by TEM; and neither did hybrid mixtures (for example, C4A + C4BK). Nonetheless, like the individual and mixtures of the arginine-based peptides, the lysine variants all showed typically α-helical CD spectra. Moreover, the spectrum for the C4AK+C4BK mixture matched that for the parent c4a + c4b mixture recorded in 300 mM salt (i.e., where fibers were not observed), Figure 3C. Similarly, the low-speed AUC experiment, Figure 4C, showed no loss in signal upon mixing C4AK and C4BK, indicating that there were no large aggregates present in this system. Finally, in the high-speed equilibrium-sedimentation experiments, Figure 5C, single ideal species fits to the data sets for C4AK, C4BK, and the mixture returned masses of 3844, 4599, and 8635 Da, respectively. In comparison, the calculated masses of C4AK, C4BK, and the theoretical heterodimer and averaged trimer are 3533, 3530, 7063, and 10594 Da, respectively. Therefore, while the individual peptides associate to some degree, the mixtures associate to a species close to, but slightly heavier than, a dimer.

In summary for this section, while the lysine-based peptides are competent for helical folding and association to extents comparable to thaose observed for the parent, arginine-containing peptides, they do not form fibers under any of the conditions tested. This emphasizes the prominent role played by arginine in intercoiled-coil interactions, presumably through multidentate

(43) Krimm, S.; Bandekar, J. *Adv. Protein Chem.* **1986**, *38*, 181–364.
(44) Tamm, L. K.; Tatulian, S. A. *Q. Rev. Biophys.* **1997**, *30*, 365–429.
(45) Heimburg, T.; Schunemann, J.; Weber, K.; Geisler, N. *Biochemistry* **1999**, *38*, 12727–12734.
(46) Musafia, B.; Buchner, V.; Arad, D. *J. Mol. Biol.* **1995**, *254*, 761–770.
(47) Kumar, S.; Nussinov, R. *Biophys. J.* **2002**, *83*, 1595–1612.
(48) Gakhar, L.; Malik, Z. A.; Allen, C. C. R.; Lipscomb, D. A.; Larkin, M. J.; Ramaswamy, S. *J. Bacteriol.* **2005**, *187*, 7222–7231.
(49) Xu, G.; Liu, R.; Zak, O.; Aisen, P.; Chance, M. R. *Mol. Cell. Proteomics* **2005**, *4*, 1959–1967.
(50) Ryadnov, M. *Angew. Chem., Int. Ed.* **2007**, *46*, 969–972.

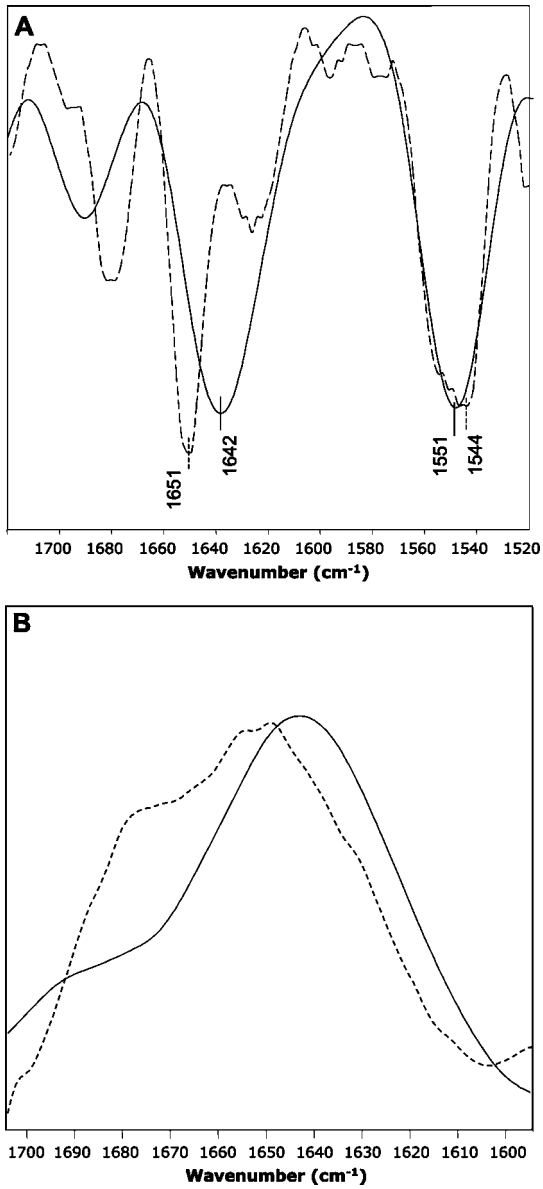

Figure 6. ATR-FTIR spectra of the SAF-pSC binary systems. (A) Second derivatives showing the typical α-helical associated peaks, 1640 and 1660 cm^{-1} (amide I band) and 1540–1550 cm^{-1} (amide II). (B) Amide I region fitted with multicomponent models, composed of peaks centered at 1631, 1649, 1691, and 1718 cm^{-1} for C4A + C4B; 1628, 1651, and 1679 cm^{-1} for C3A + C3B. Key: C4A + C4B (solid line), and C3A + C3B (broken line).

salt-bridged networks that operate at both the intra- and intercoiled-coil levels.

Conclusion

In summary, we have constructed four pairs of peptides that combine previously described principles for the design of sticky ended leucine zippers (LZs), which foster fibrillogenesis to long α-helical coiled coils, with the straightforward idea of covering the outer faces of the coiled coils with charged side chains. The aim was to improve the solvation of the fibers, and thus limit their maturation and thickening into stiff rods. This yields fibers that are considerably thinner (down to ~10 nm in diameter) than those of foregoing designs. Interestingly, the thinned fibers are also more flexible than previously described fibers. As a result, the new fibers entwine and wrap around each other—although they do not gel at the concentrations examined (≤200 μM peptide)—whereas previous designs form stiff rods with very long persistence lengths. In order to accommodate the supercharged surfaces, basic and acidic residues were combined along the outer faces of the coiled coils in *i*, *i*+3 and *i*, *i*+4 arrangements compatible with α-helical geometry. This brings another property to the system: all of the peptides, both individually and when mixed, tend to fold to α-helical structures even under conditions that do not lead to full fibrillogenesis. Furthermore, these soluble helical assemblies are associated into small aggregates, which are probably mixtures of monomers, dimers, and trimers. These properties of the soluble peptides probably reflect the strong propensities of the designed sequences to form α-helical LZs. We note that this presents possibilities for studying the early events in peptide fibrillogenesis, which will be explored elsewhere. Finally, we observe that full assembly into fibers is only achieved in this system by using ariginine as the basic residue and not lysine. Presumably, and consistent with other systems,[50] this reflects the need to make both intrahelical and intercoiled-coil interactions in fibers, Figure 2. With lysine, the options are limited, but arginine allows both types of interaction to be made at each basic side chain. The importance of intercoiled-coil−salt-bridge interactions is also reflected in the disruption of fiber formation by salt, which does not affect the α-helical folding of the peptides.

In conclusion, this work demonstrates further the ability to program the sequences of fiber-forming peptides to alter the size, shape, and stiffness of the resulting fibers. In this case, we covered the outer faces of long, coiled coils fully with charged residues to reduce previously observed fiber thickening and stiffening. We posit that such "smears of mixed charge (anionic plus cationic)", as opposed to "discrete charged patches (anioinic or cationic)" described previously,[20,24] allow better solvation of the coiled-coil fibrils, which leads to less bundling and, thence, less order and stiffening. This work provides another step toward the rational design of peptide-based fibrous biomaterials from the bottom up; specifically, toward the goal of making fibers, matrices, and networks of tailored dimensions and morphology, and with prescribed physical properties.

Acknowledgment. We thank the BBSRC and the EPSRC of the U.K. for financial support (Grants BBS/B/04676 and GR/T09224/01), and Charl Faul and the DNW group for valuable discussions.

Supporting Information Available: Experimental Section. This material is available free of charge via the Internet at http://pubs.acs.org.

JA0778444